

# Change of the Tropical Hadley Cell Since 1950

*Xiao-Wei Quan, Henry F. Diaz, and Martin P. Hoerling  
NOAA-CIRES Climate Diagnostic Center, Boulder, Colorado, USA*

*last revision: March 24, 2004*

## **Abstract**

The change in the tropical Hadley cell since 1950 is examined within the context of the long-term warming in the global surface temperatures. The study involves analyses of observations, including various metrics of Hadley cell, and ensemble 50-year simulations by an atmospheric general circulation model forced with the observed evolution of global sea surface temperature since 1950. Consistent evidence is found for an intensification of the Northern Hemisphere winter Hadley cell since 1950. This is shown to be an atmospheric response to the observed tropical ocean warming trend, together with an intensification in El Niño's interannual fluctuations including larger amplitude and increased frequency after 1976. The intensification of the winter Hadley cell is shown to be associated with an intensified hydrological cycle consisting of increased equatorial oceanic rainfall, and a general drying of tropical/subtropical landmasses. This Hadley cell change is consistent with previously documented dynamic changes in the extratropics, including a strengthening of westerly atmospheric flow and an intensification of midlatitude cyclones.

## **1. Introduction**

The tropical Hadley cell, by definition, is the zonal mean meridional mass circulation in the atmosphere bounded roughly by 30°S and 30°N. It is characterized by equatorward mass transport by the prevailing trade wind flow in the lower troposphere, and poleward mass transport in the upper troposphere. This lateral mass circulation links the mean ascending motion in the equatorial zone with subsidence in the subtropics, and represents a major part of the large-scale meridional overturning between tropics and subtropics. In this paper we will examine the long-term change of the tropical Hadley cell as an expression of climate change associated with a warming trend in global mean surface temperature during the last half-century (IPCC, 1996, 2001).

Previous observational studies have confirmed that the global annual mean surface temperature has increased about 0.6 °C during the past century (e.g., Jones et al. 1999). The warming has occurred in a step-like manner having two phases, one from about 1910 to 1945, and a second after the mid-1970s. Recent observational studies of the global pattern of temperature changes have revealed that, since the late 1970s, the warming trend in global land surface air temperature (LSAT) is larger than the warming trend in sea surface temperature (SST) (IPCC, 2001). The recent temperature changes over the land-masses of the northern midlatitudes during winter appears related to changes in atmospheric circulation (e.g. Hurrell 1996; Gaffen, et al. 2000; Parker 2000;

Santer, et al. 2000). Pronounced changes in the wintertime atmospheric circulation have occurred since the mid-1970s over the Northern Hemisphere. The variations over the North Atlantic are related to changes in the North Atlantic Oscillation (NAO), and the changes over the North Pacific involve variations in Aleutian low with teleconnections downstream over North America.

To what extent are these changes in subtropical and midlatitude circulation systems linked to a tropical source, rather than being a mere expression of intrinsic extratropical climate noise? And furthermore, are these circulation changes an indication of the atmospheric response to an intensified tropical Hadley cell? There is evidence for an intensification in marine surface wind since 1950, as recorded by observations from ships sailing over the global oceans (Diaz et al. 1992, 1994). The intensification in the observed ship-based marine surface wind is most significant in their zonal (east/west) component during the northern winter since the late 1970s. The intensification of the northern winter zonal wind partially reflects the intensification of the Aleutian Low and prevailing westerlies over the mid-latitude central and eastern Pacific (e.g. Trenberth and Hurrell, 1994; Graham, 1994), and the strengthening of mid-latitude westerly winds over the North Atlantic Ocean associated with a trend of the North Atlantic Oscillation (NAO) toward its positive phase (e.g. Hurrell, 1995; Thompson et al. 2000). Observational studies also find that since 1948, the frequency and intensity of extreme cyclones has increased markedly over the North Pacific Ocean during northern winter (Graham and Diaz, 2001).

It has also been argued that the intensification of the extratropical northern winter circulation is a result of increasing ocean surface temperature, particularly in the tropics (e.g. Hoerling et al. 2001a for the tropical origins of the NAO change; and Graham et al. 1994; Lau and Nath 1994, 1996 for the tropical forcing of changes over the North Pacific). Model simulations indicate that the atmospheric angular momentum increases in response to a warming of tropical SST, and there is an indication that the observed atmospheric angular momentum has itself increased since 1950 (Huang et al. 2001, 2003). Increasing angular momentum (i.e., increasing westerly flow) can be due to a strengthened tropical Hadley cell and/or increased eddy forcing from midlatitude. That an intensified Hadley cell due to diabatic forcing may be particularly relevant is implied by model evidence for a substantial increase in zonal mean equatorial rainfall since 1950 (Kumar et al. 2004), which would lead a stronger mean ascending branch of the Hadley cell. Such changes in diabatic heating are consistent with the overall tropical SST warming (Hurrell et al., 2004).

A significant component of the warming trend in the global ocean (Levitus et al. 2000) has been the strong warming in the tropical ocean during recent decades (e.g. Lau and Weng 1999). As shown in Figure 1, since 1950, strong warming in the tropics has occurred in the Indian Ocean, the western Pacific, along the coasts of Southeast Asia, off equatorial Indonesia, and the Atlantic Ocean. The origins for these warming are still under investigation, though the Indo-west Pacific warming has been argued to be inconsistent with intrinsic unforced coupled ocean-atmosphere interaction alone (Knutson, et al. 1999).

The tropical Indian and western Pacific Oceans possess the warmest water in the global ocean, with SST often higher than 28°C, and this is usually being referred to as the “warm-pool” region. Because of the already warm surface, atmospheric convection is

sensitive to small temperature changes in the warm-pool region. It is interesting to note that the warming in the warm-pool region has occurred in a manner that is somewhat

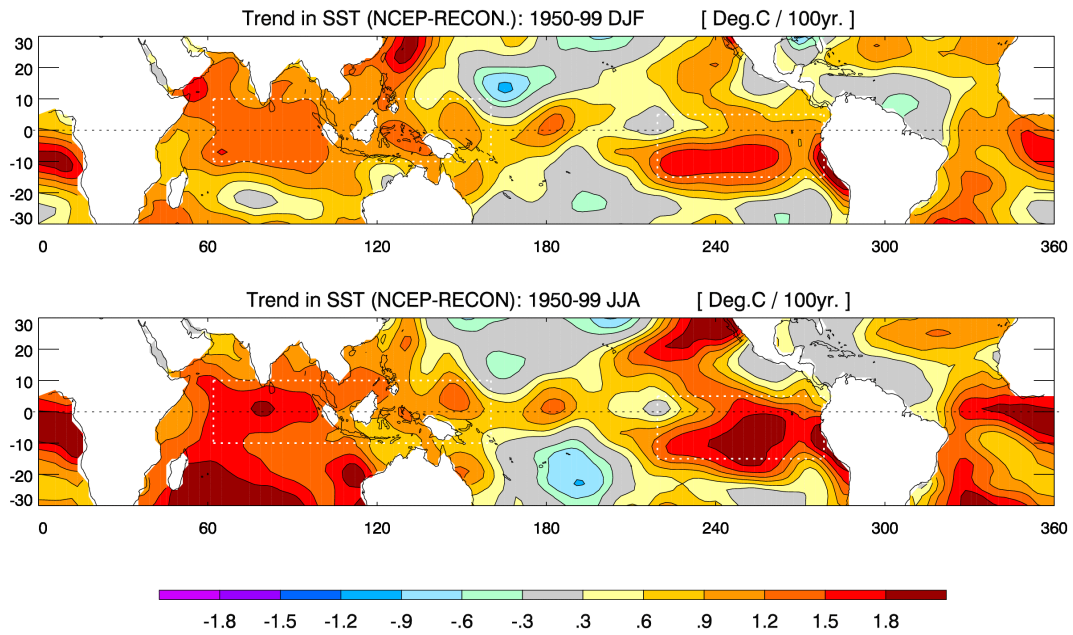


Figure 1. Spatial distribution of the linear trend of tropical SST. The data used are from Smith and *et al.* (1996).

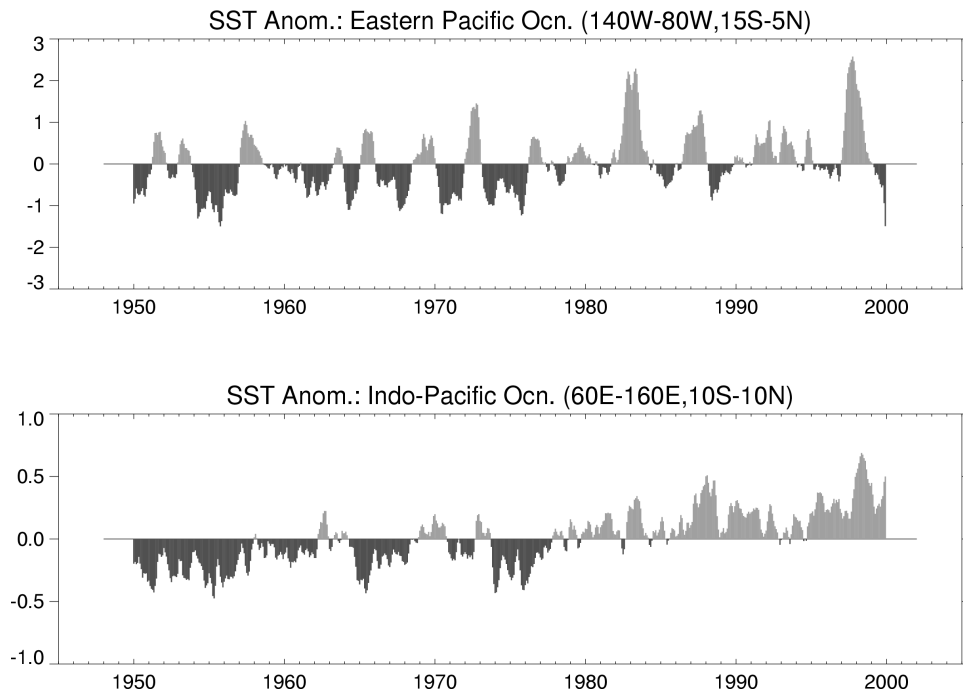


Figure 2. Time series of spatial mean SST anomalies with respect to 1950-99 climatology.

different from the warming in the eastern tropical Pacific. The SST in the tropical Indian and west Pacific region has been increasing since 1950 with a step-like increase in the late 1970s (lower panel in Fig. 2). This change is large compared to the small natural variability (Latif et al. 1997), suggesting it is consistent with the notion that the warming has been externally forced (Hoerling et al. 2004).

The manner in which the atmospheric circulation has adjusted to such changes in the tropical oceans is still an open question. Recent satellite observations indicate that the tropical Hadley cell has been strengthening (e.g. Chen et al., 2002), but others argue that the signal of the change in the Hadley cell is not large enough to exceed the range of uncertainty in current observational systems (e.g. Trenberth, 2002). In this paper, we analyze the temporal evolution of the tropical Hadley cell since 1950. An analysis on longer-term change in the tropical Hadley cell based on marine surface wind observations can be found in Evans and Kaplan (2004, this volume). Data used for the analyses in this paper are described in section 2. The long-term change of the Hadley cell contained in observational data are examined in section 3, followed by analyses on the change of the Hadley cell in atmospheric model simulations in section 4. Conclusions and further discussions about the nature of the long-term change of the Hadley cell are given in section 5.

## 2. Data

Three independent data sets are used in this study. The monthly mean data of the NCEP/ NCAR reanalysis (Kistler et al. 2001) covers the period from January 1948 to present. Values of monthly mean zonal and meridional (north/south) wind components are available at 17 pressure levels at  $2.5^\circ$  longitude by  $2.5^\circ$  latitude grid-points. The NCEP/ NCAR reanalysis data is not a purely observed data set. It is a mix of real observations with model simulations using the method of temporal and spatial assimilation in an atmospheric general circulation model (AGCM). Insofar as different data platforms have been used in construction of the reanalysis, long-term trends calculated from it may be non-physical.

In order to clarify whether the change of the tropical Hadley cell diagnosed from the reanalysis data is a physical signal of true climate change, we also analyze an ensemble of 50-year AGCM simulations. The ensemble includes 10 simulations of an AGCM developed at the European Center for Medium Range Weather Forecast (ECMWF) and Max-Planck Institute at Hamburg, ECHAM-3 (Roeckner et al. 1992). All of the 10 simulations were identically forced with the observed monthly global SST evolution from 1950 to 1999, and the 10 simulations differ from each other by starting from different initial conditions. Simulations of the monthly mean precipitation, 850-hPa, and 200-hPa wind fields, are analyzed. The spatial resolution of the model experiments is about  $2.8^\circ$  longitude by  $2.8^\circ$  latitude.

The third data set is the satellite-rain gauge combined precipitation dataset produced by the Global Precipitation Climatology Project (GPCP, cf. Huffman et al. 1997). The GPCP precipitation data are available in the form of monthly means on  $2.5^\circ$  by  $2.5^\circ$  grid points, and covers the period from 1980 to present.

### 3. Change of the tropical Hadley cell in the NCEP reanalysis

#### 3.1 Climatology of the Hadley cell

A conventional way to depict the tropical Hadley cell is to use the streamfunction of zonal mean meridional and vertical velocity in the meridional-vertical plane (e.g. Oort and Yienger 1996). The 1950-99 long-term average of the annual mean and also the seasonal cycle of the streamfunction in the NCEP/NCAR reanalysis, are shown in Figure 3. As represented by the contour-lines of the annual mean streamfunction (top panel in Fig. 3), the tropical Hadley cell is a major component of the global mass circulation, which consists also of the Ferrel cell in midlatitudes, and the polar cell in high latitudes. In the annual mean climatology, there are two Hadley cells in the tropics, one on each side of the equator, and both are much more intense than the Ferrel and polar cells in the extratropics. The annual mean tropical Hadley cell in the Southern Hemisphere (SH) is stronger than its counterpart in the Northern Hemisphere (NH), and the dividing latitude of the two Hadley cells roughly corresponding to the latitude of mean ascent, is located north of the equator, reflecting the fact that the inter-tropical convergence zone (ITCZ) remains in the NH throughout the year. A comprehensive review of the issues regarding the position of the ITCZ is given by Xie (2004) in this volume. An analysis of the biases in previous calculations of the Hadley circulation using in-situ rawinsonde data can be found in the paper by Waliser *et al.* (1999).

The tropical Hadley cells vary strongly with the change in seasons. For example, the ascending branch of the Hadley cell migrates seasonally across the equator in response to the solar annual cycle, and the structure (for instance, the polarity, and single versus double cell) of the tropical Hadley cell adjusts accordingly. A study by Dima and Wallace (2003) shows that the seasonal cycle of the climatological mean tropical Hadley cells is dominated by two components of roughly comparable amplitude: a seasonally invariant pair of Hadley cells with rising motion centered near and just to the north of the equator and subsidence in the subtropics (e.g. the Hadley cells of annual mean, MAM, and SON in Fig. 3); and a seasonally reversing, solstitial cell with ascent in the outer tropics of the summer hemisphere and subsidence in the outer tropics of the winter hemisphere (e.g. the Hadley cells of DJF and JJA in Fig. 3). The seasonality of the tropical Hadley cell represents only part of the much stronger seasonality and regional migration of the monsoons systems over Asia and the Americas (e.g. Webster 1987; Philander, 1990; Trenberth et al. 2000; Webster, this volume).

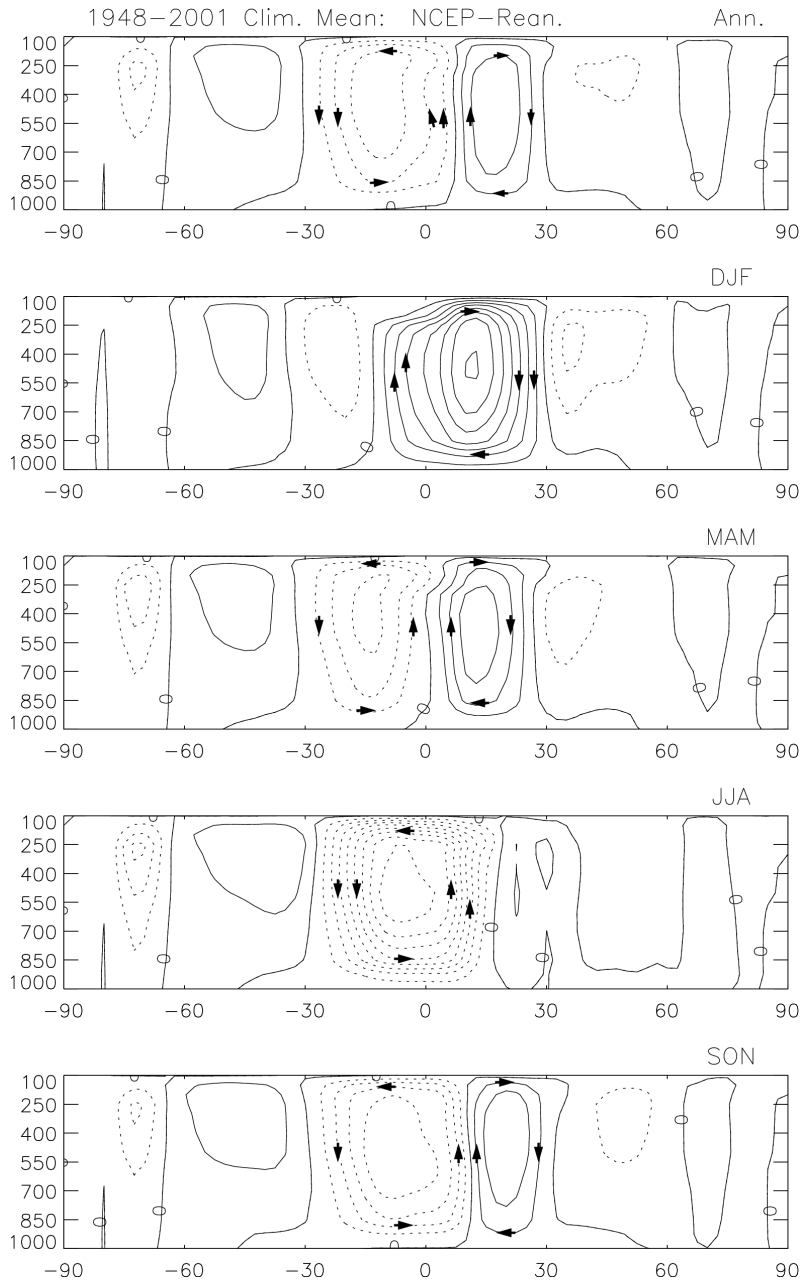


Figure 3. Streamfunction of the zonal mean meridional wind circulation based on the NECP reanalysis. Units are in  $10^{10} \text{ kg s}^{-1}$  and the contour interval is  $2 \times 10^{10} \text{ kg s}^{-1}$ .

### 3.2 Interannual variability in the Hadley cell

The interannual variability of the tropical Hadley cell is dominated by the ocean-atmosphere variability associated with ENSO. This connection has previously been illustrated by composite methods that difference the mean state of the Hadley cell during the warm phase of ENSO from its cold phase counterpart. Such composite differencing extracts the linear component of the Hadley cell's response. Oort and Yienger (1996) applied this method to radiosonde observations and found that the Hadley cell's linear

response to ENSO consists of a pair of anomalous direct meridional cells symmetric about the equator. Their analysis indicates that the two anomalous cells are strengthened (weakened) during El Niño (La Niña) events.

Using the same methodology, the composite linear response of the Hadley cell to ENSO in the NCEP/NCAR reanalysis data is shown in the top panel in Figure 4. The years included in the composite are listed in Table 1. Waliser et al. (1999) indicated differences in structure exist between the radiosonde-based and the reanalysis-based composites, and they also noted that the composite linear response in the reanalysis is weaker than that in the radiosonde data. Their analysis also showed that the differences between the two composites are largely attributed to the sparse spatial coverage of the in-situ data. Nevertheless, our results are in qualitative agreement with that of Oort and Yienger (1996) in so far as the linear El Niño signal during northern winter consists of anomalous ascent located south of the equator, with subtropical sinking in both hemispheres. In contrast to the results of Oort and Yienger (1996), our analysis also shows a secondary anomalous southward overturning meridional cell extending from about 15° to 30° N, and shows a stronger anomalous circulation in the upper troposphere.

*Table 1.* List of El Niño and La Niña event years (1950-2002) used in the composite analysis. The year is considered El Niño (La Niña) when the DJF Niño-3.4 SST index exceeds (+/-) 1 standard deviation.

---

El Niño	La Niña
1958	1951
1966	1955
1969	1956
1973	1965
1983	1971
1987	1974
1992	1976
1995	1985
1998	1989
	1999
	2000

---

We present new evidence that the nonlinear component of the Hadley cell's response to ENSO is comparable to the linear signal. The nonlinear component is defined here as the sum of Hadley cell anomalies for El Niño and La Niña. In the case that these anomalies are of exactly equal amplitude but opposite polarity, the nonlinear component would be judged to be zero. Figure 4 compares the composite anomalous Hadley cell pattern for the El Niño events (Fig. 4, 2nd panel from top) with its counterpart for the La Niña events (Fig.4, 3rd panel from top). The two composites are different in two aspects: (1) the composite of the anomalous Hadley cell shows stronger response to the El Niño

than the La Niña events, and (2) the anomalous Hadley cell for the El Niño events is characterized by a single strong anomalous cell over the equator, while a near-equatorial anomalous Hadley cell during La Niña events is virtually absent. This non-linearity is further illustrated in the bottom panel in Figure 4, which shows the sum of the composites for El Niño and La Niña events. It is clear that the one-cell structure in the nonlinear response of the Hadley cell to ENSO extreme phase is comparable to its linear signal (Fig. 4, top panel).

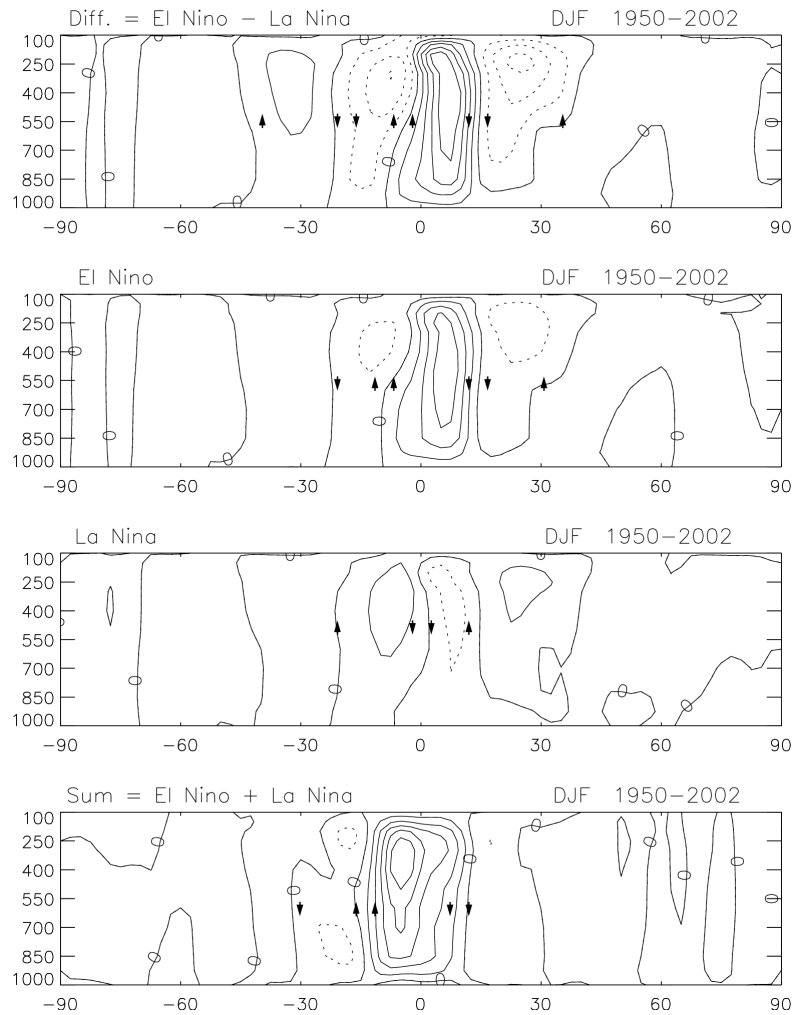


*Figure 4.* Difference in the anomalous zonal mean meridional streamfunction between El Niño and La Niña periods (top panel). The composite anomalous pattern of the zonal mean meridional streamfunction for El Niño (the 2nd panel from top) and La Niña (3rd from top) periods. And the sum of the two composites (bottom panel). Contour intervals are  $4 \times 10^9 \text{ kg s}^{-1}$  in the top three panels, and  $2 \times 10^9 \text{ kg s}^{-1}$  in the bottom panel.

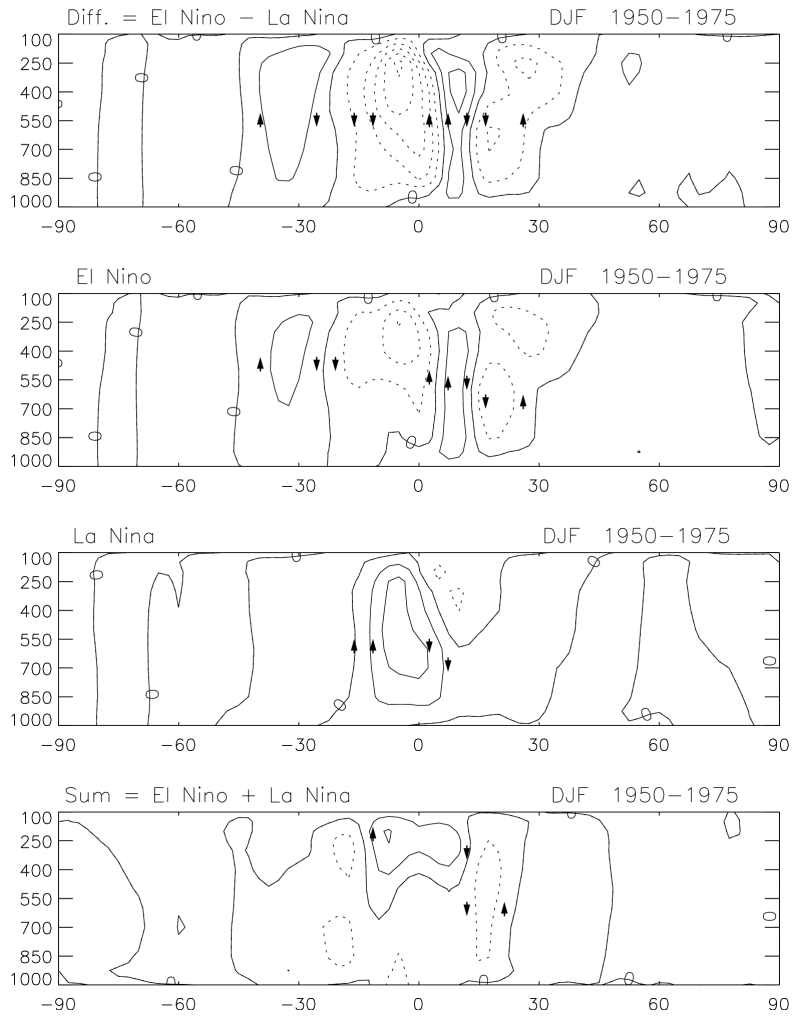


Figure 5 Difference in the anomalous zonal mean meridional streamfunction between El Niño and La Niña events (top panel) during the period of 1950–75. The composite anomalous pattern of the zonal mean meridional streamfunction for El Niño (2nd panel from top) and La Niña (3rd from top) periods, and the sum of the two composites (bottom panel). Contour intervals are  $4 \times 10^9 \text{ kg s}^{-1}$ .

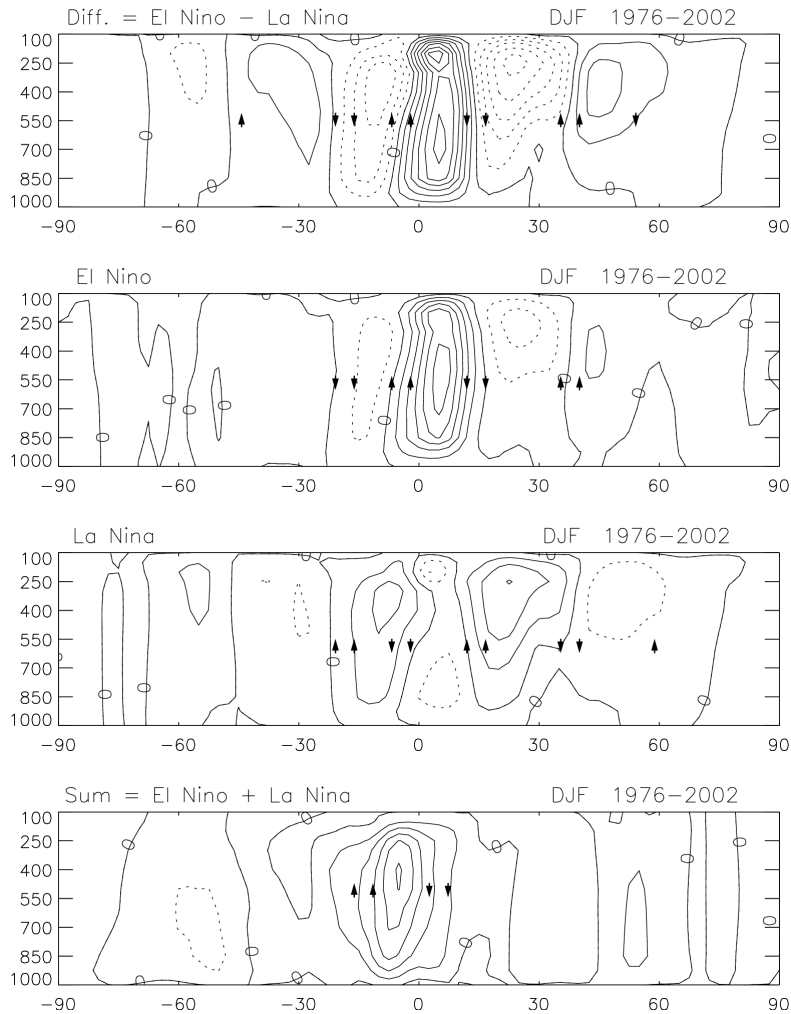


Figure 6. Same as Fig. 5, but for the period of 1976-2002.

We further examine the composites for the sub-periods of 1950–75 and 1976–2002 in Figures 5 and 6, respectively, to assess robustness of ENSO signal in the Hadley cell. The composite patterns are obtained using the same method as that used for Figure 4, except that all the anomalies in Figure 5 and 6 are based on the climatological mean for the 1950–75 and 1976–2002 period, respectively. The purpose of using different climatologies for the two shorter periods is to reduce the effect of any possible artificial change in the climate mean state in the reanalysis data as discussed in section 2. The linear signals are qualitatively similar for the two periods, though with stronger amplitude in recent decades (top panels in Fig. 5 & 6). The nonlinear component in the Hadley cell’s responses to ENSO is virtually absent in the composite of 1950–75, and is apparent in the 1976–2002 period (bottom panel in Fig. 6). This is mainly due to an interdecadal change in the tropical Hadley cell’s response to the warm events. The Hadley cell had responded to the El Niño events with a largely intensified southward overturning anomalous cell and a slightly increased northward overturning anomalous cell before 1976 (2nd panel from top in Fig.5), compared to much stronger northward overturning anomalous cell with a slightly increased southward overturning cell for the El Niño

events after 1976 (2nd panel from top in Fig. 6). There is also a stronger northward overturning anomalous cell over the Northern Hemispheric subtropics for the La Niña events after 1976 (3rd panel from top in Fig. 6). It should be emphasized that these epoch differences are being estimated from small sample sizes, and thus subject to appreciable sampling error. Nevertheless, it will be shown in section 4 that similar epoch differences in the Hadley cell's responses to ENSO occur in a large ensemble of climate simulations.

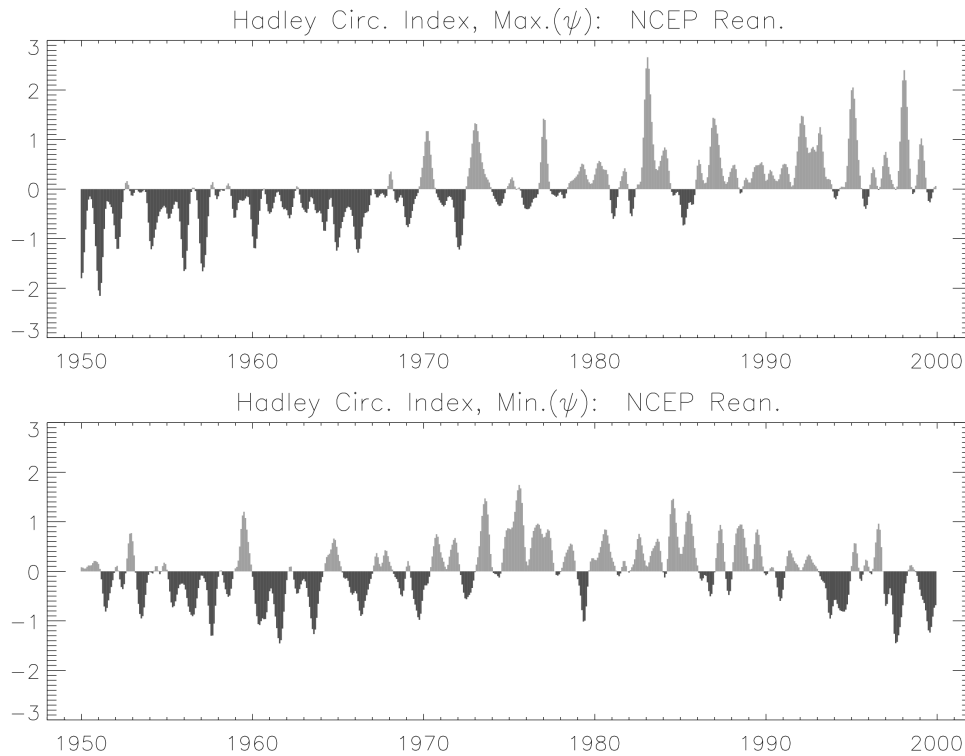


Figure 7 Time series of index for the tropical Hadley cells. Temporal variation of the northward/southward overturning cell is represented by the maximum/minimum of the zonal mean meridional streamfunction (upper/lower panel). Positive/negative values indicate stronger northward/southward overturning. The time series are smoothed with an 11-month weighted filter. Units are in  $10^{10} \text{ kg s}^{-1}$

### 3.3 Interdecadal change in the Hadley cell

In order to describe the temporal variation of the Hadley cell's intensity, we use the maximum value of the zonal mean streamfunction occurring within the latitudinal zone of  $0-30^{\circ}\text{N}$ . This measures the strength of the northward overturning Hadley cell, and the minimum value of the zonal mean streamfunction within  $0-30^{\circ}\text{S}$  measures the strength of the southward overturning Hadley cell (Oort and Yienger, 1996). Time series for the monthly mean strength of the northward and southward overturning Hadley cells are shown in Figure 7. It is interesting to note that the northward overturning Hadley cell shows a trend toward intensification throughout the past 50 years. But the southward overturning Hadley cell does not show a similar long-term trend. The southward

overturning Hadley cell shows an interdecadal swing with the index being low (i.e., intensified southward overturning) during the decades of 1950s and 1960s, high (or weakened southward overturning) during 1970s and 1980s, and low again during the 1990s. Since the northward overturning Hadley cell dominates during the northern winter, and the southward overturning Hadley cell prevails during the southern winter (Fig. 3), the difference between the long-term changes in the northward and southward overturning Hadley cells implies that the tropical Hadley cell has intensified in the northern winter but not in the southern winter. This seasonal difference in the tropical Hadley cells' long-term change is further illustrated in Figure 8 which shows the difference between the temporal average of the zonal mean meridional streamfunction for two periods: 1948–75 and 1976 to present for the annual mean, and four cardinal seasons. We have selected these two periods in light of the different Hadley cell's behaviors seen in both the reanalysis and the ensemble AGCM simulations (section 4) before and after 1975. The intensification in the annual mean Hadley cell is mainly due to the intensification of the northward overturning Hadley cell during the northern winter (DJF) and spring (MAM). The interdecadal difference in the zonal mean streamfunction for the two periods appears to be very small during the northern summer (JJA) and autumn (SON).

To further diagnose the structure, in addition to the amplitude, of the variation in the tropical Hadley cells since 1950, we calculate the vertical shear of the zonally averaged meridional velocity between 200 hPa and 850 hPa. This depiction of the tropical Hadley cells is illustrated in Figure 9, in which the close correspondence between the seasonal reversal of the solstice Hadley cell and the change of the vertical shear in the zonal mean meridional wind can be clearly seen.

Since the long-term changes in the tropical Hadley cell during the northern winter and spring are quite different from their counterpart during the northern summer and fall, it is necessary to separately examine the long-term Hadley cell's change for winter and summer. The temporal variation in the zonal distribution of the upper-minus-lower anomalous meridional wind is examined for JJA and DJF, respectively, in Figure 10. This diagnosis of the long-term change of the tropical Hadley cell is consistent with the results from the analysis based on the zonal mean meridional streamfunction.

Both the long-term trend toward intensification in the winter/northward overturning Hadley cell, and the interdecadal swing in the change of the summer/southward overturning Hadley cell, as depicted in Fig. 7 & 8, are seen clearly also in Figure 10.

There is an apparent “regime change” of the northern winter Hadley cell occurring in the mid-1970s, which has three elements. First, the Hadley cell was generally weaker in the early decades. Second, the interannual pulses of the Hadley cell before mid-1970s were weaker compared to the pulses of the Hadley cell after then. And third, the Hadley cells have been responding to the warm ENSO phase with an intensified northward overturning cell during the later period.

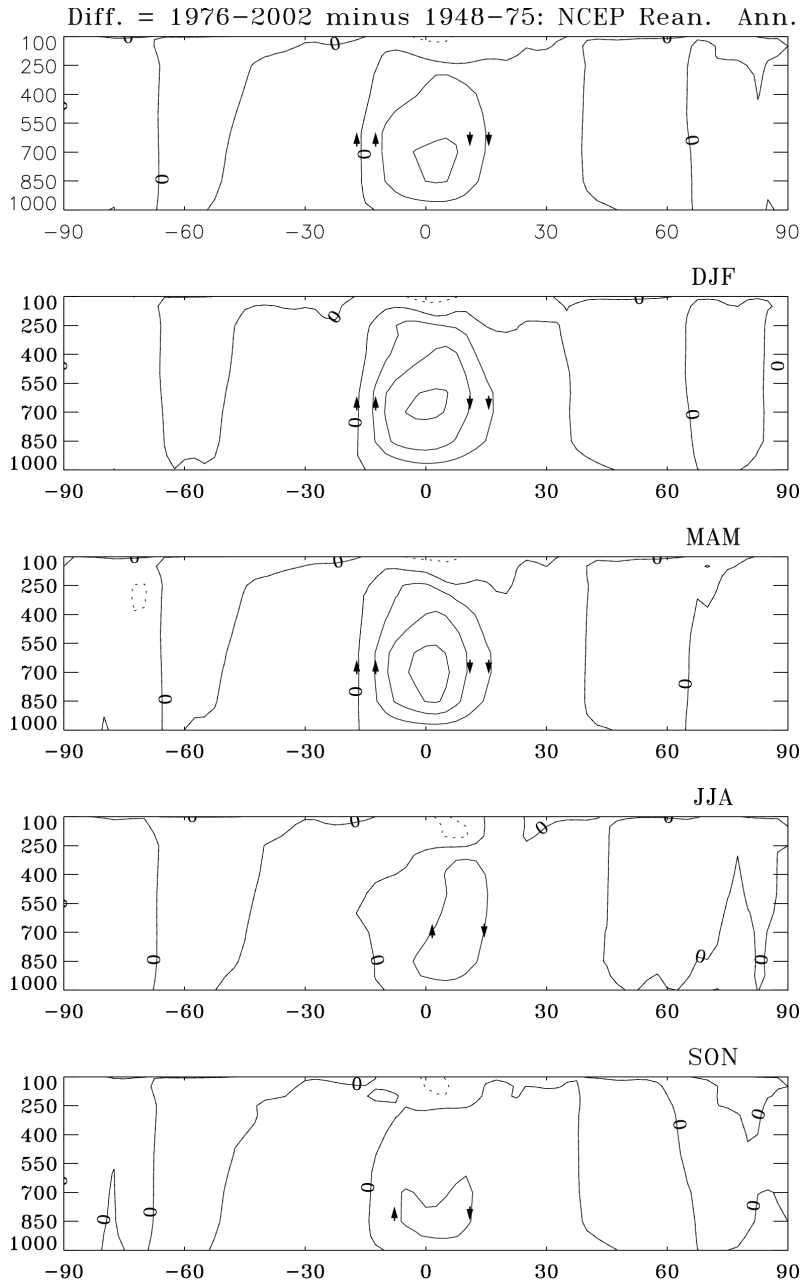


*Figure 8.* Difference in the time-averages of the zonal mean meridional streamfunction in the NCEP/NCAR reanalysis: the average of 1976–2002 minus the average of 1950–1975. Contour intervals are  $2 \times 10^{10} \text{ kg s}^{-1}$

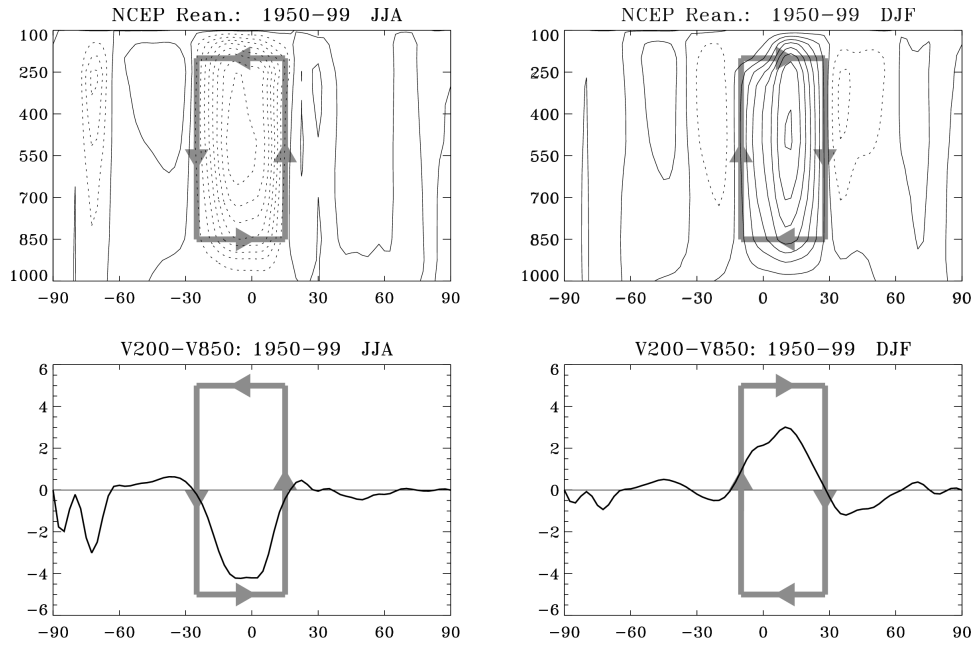


*Figure 9.* Climatological mean of the zonal mean meridional streamfunction (upper two panels), and the difference between the zonal mean of the meridional wind at 200 hPa and 850 hPa (lower two panels) for JJA and DJF. The difference is obtained by subtracting the 850 hPa meridional wind value from the 200hPa wind value at each latitudinal grid-points.

To further clarify the apparent regime change in the atmospheric circulation over the tropical Pacific, we have also examined the spatial distribution of the tropical rainfall anomalies during the warm ENSO events for the two sub-periods. These have been extracted from the reanalysis data, and should be viewed with caution since that data did not assimilate observed gauge rainfall estimates. Figure 11 shows the comparison of the composite anomalous rainfall pattern for the winter (DJF) of El Niño events during the 1950-1968 period, against its counterpart during the 1976–2002 period. During the earlier period, the anomalous rainfall pattern during El Niño events is characterized by a belt of increased rainfall over the tropical Pacific located mostly on the north side of the equator. In contrast, the belt of increased rainfall over the tropical Pacific has shifted largely to the south side of the equator during the warm ENSO events since 1976. There is thus some indication that the interdecadal change in the anomalous rainfall belt over the tropical Pacific is consistent with the interdecadal change in the tropical Hadley cells' response to the warm ENSO events. Further discussion is found in section 4.3.

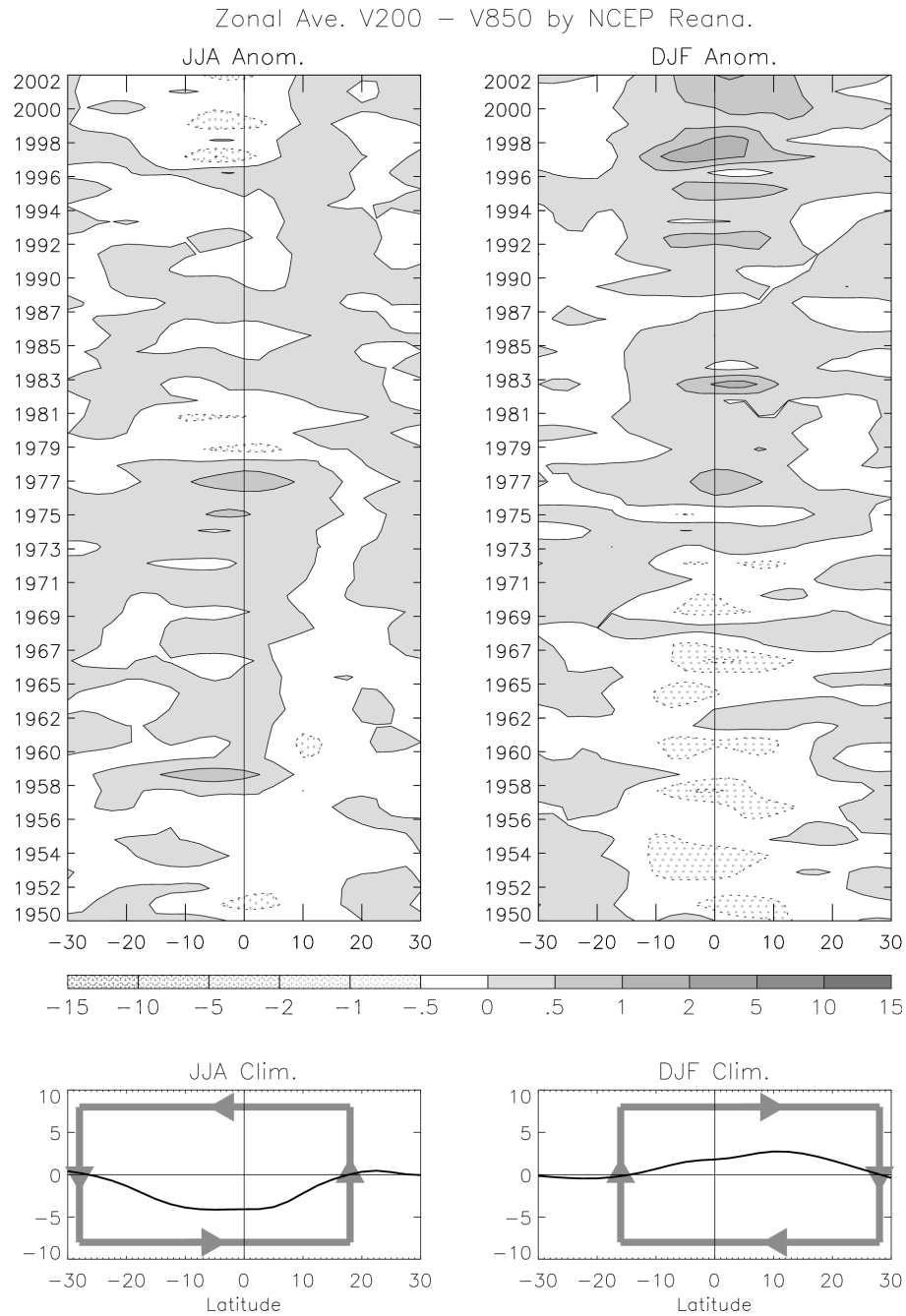


*Figure 10.* Time-latitude cross-section of the anomalous zonal mean vertical shear between the meridional wind at 200 hPa and 850 hPa (V200 minus V850) in the NCEP/NCAR reanalysis for JJA and DJF, respectively. The climatological means of the zonal mean vertical wind-shear for JJA and DJF are shown in the bottom two panels with the schematic arrows interpreting the meaning of the positive/negative signs of the values.

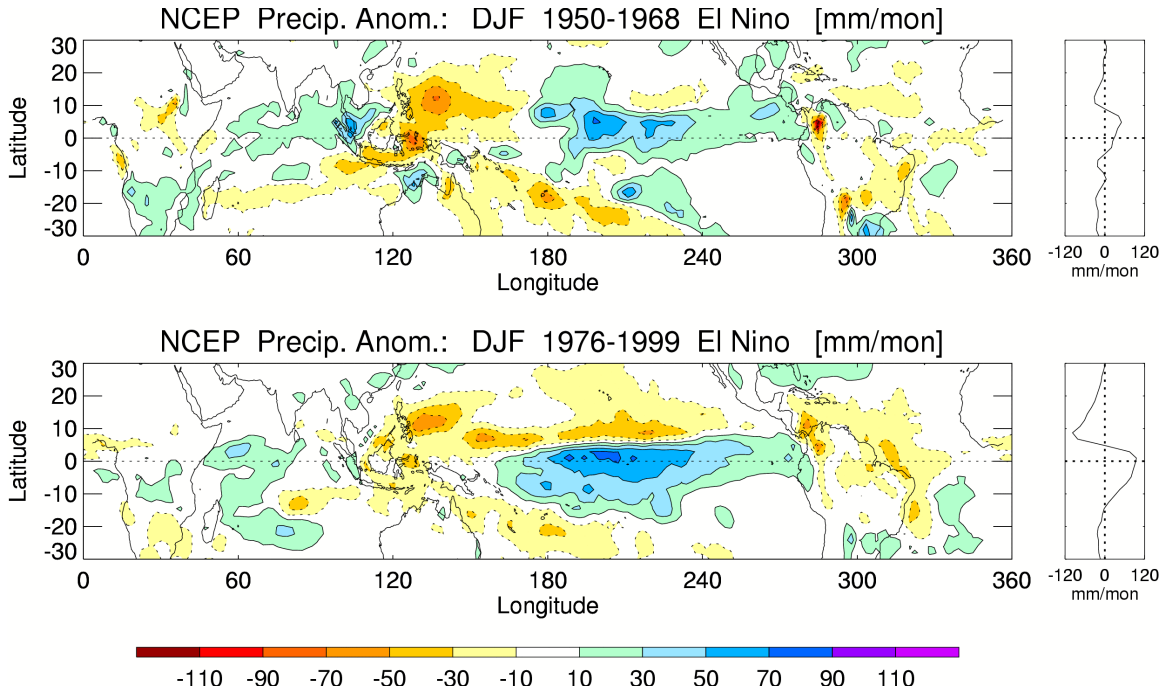


Figure 11. Composites of the anomalous precipitation in the NCEP/ NCAR reanalysis during the winter (DJF) of El Niño events in the 1950–1968 (top panel) and 1976–2002 (bottom panel) periods. Zonal means of the anomalous precipitation are shown in the panels on the right-hand side.

#### 4. Change of the tropical Hadley cell in AGCM simulations

##### 4.1 Validation and attribution of the observed Hadley cell change

An important question is whether the temporal evolution of the tropical Hadley cell since 1950 shown in the NCEP/NCAR reanalysis data is physical, and consistent with an atmospheric response to the forcing by changes in SST. To address this question, we apply the same analysis to ensemble AGCM simulations and compare 1950–1999 temporal evolution of the model simulations with those in the reanalysis data. A similarity between the change in the ensemble model simulations and that found in the reanalysis data would provide some justification for claiming the existence of a forced signal, and that the effect of artificial climate shifts in the reanalysis data due to non-physical processes of data input changes is minimal.

Ensemble averages of the model simulated temporal variation of the vertical shear between 200 hPa and 850 hPa zonal mean meridional wind for the past five decades are shown for DJF and JJA in Figure 12. Three major features of the simulated variation of the tropical Hadley cell are similar to those seen in the NCEP/NCAR reanalysis (Fig. 10). (1) An intensification of the northward overturning Hadley cell during the Northern Hemispheric winter (DJF) in recent decades, (2) a strong ENSO signature in the interannual variations of the simulated Hadley cell, and (3) little long-term trend in the southward overturning Hadley cell in the Northern Hemisphere summer (JJA). As in the

observations, there is evidence for a regime-change in the behavior of the northern winter Hadley cell, though occurring later in the AGCM. Thus, the simulated Hadley cell is weaker in the 1950s, 60s and 70s compared to later decades, and more intense interannual variations are seen after 1976.

The regime change related to ENSO induced rainfall patterns is shown in Figure 13, which compares composites of the tropical rainfall anomalies for the El Niño events during the 1950-68 and 1976-99 periods, respectively. Similar to the reanalysis data (Fig. 11), increased rainfall over the tropical Pacific Ocean occurs mostly north (south) of the equator during the ENSO events of earlier (later) decades. Particularly evident is the increased spatial coverage of equatorial enhanced rainfall during recent El Niño events.

Hadley Circulation Index: Zonal Ave. V200 – V850 by ECHAM3

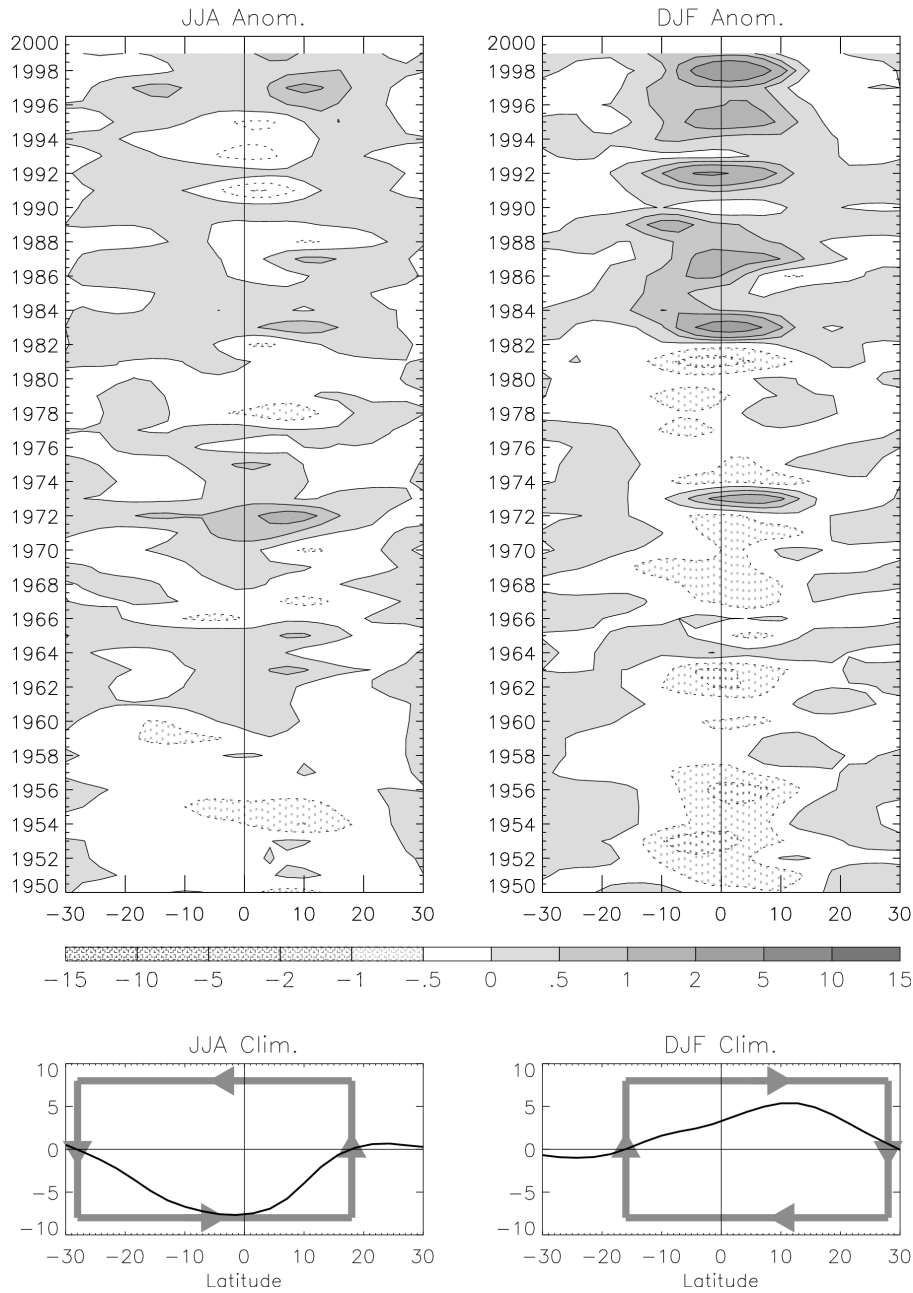


Figure 12 Same as Fig. 10, but for the ensemble mean of the ECHAM3 simulations.

Based on the qualitative agreement between the time history of simulated and the reanalysis Hadley cell intensities, we propose that the change in Hadley cell strength during the northern winter is consistent with an oceanic change. To the extent that the relevant oceanic changes are not themselves forced by the Hadley cell, then the trend in the Hadley cell is judged to have been forced by the oceans as revealed in these AGCM simulations.

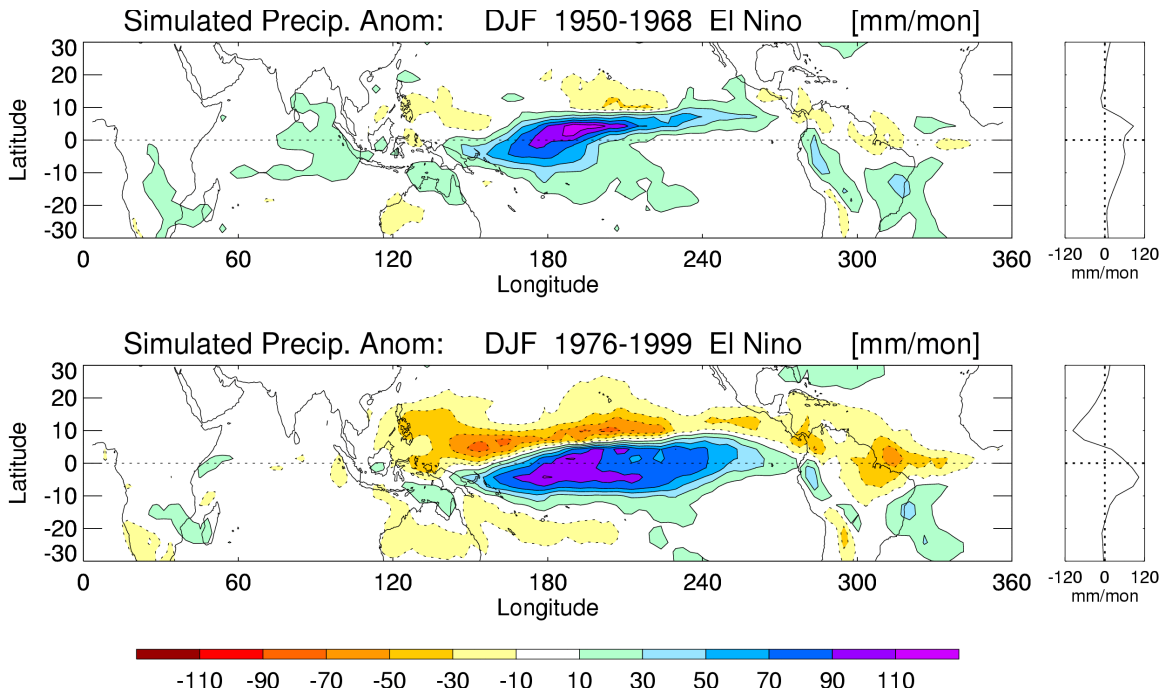


Figure 13. Same as Fig. 11, but for the ensemble mean of the ECHAM3 simulations.

#### 4.2 The seasonal dependence of the interdecadal change in the tropical Hadley cell

The seasonal dependence of the interdecadal change in the tropical Hadley cell is further examined in Figure 14, which shows the time series of the vertical shear of the 200- hPa minus 850-hPa zonal mean meridional wind at the equator for DJF and JJA, respectively. The DJF time series shows an increasing trend of about 0.02 m/s per year. The differences among the 10 simulations are relatively small (indicated by the vertical distance between the dashed lines and the solid lines in their outer side in Fig.14). On the other hand, the JJA time series does not show a significant trend during the 50-year period, and has larger sample-to-sample differences among individual simulations.

The seasonal dependence of the simulated change in the Hadley circulation since 1950 appears to reflect different impacts of the SST warming on the oceanic-dominated monsoons during boreal winter versus the continental-dominated monsoons during boreal summer. During winter, a warming of the oceans throughout the deep tropics yields an increase in zonally averaged rainfall, and hence an intensification of the zonally symmetric meridional overturning (Figure15, top panel). The simulated summertime rainfall trend is more regional, and lacks a zonally symmetric component, especially in the southern tropics (Figure 15, bottom panel).

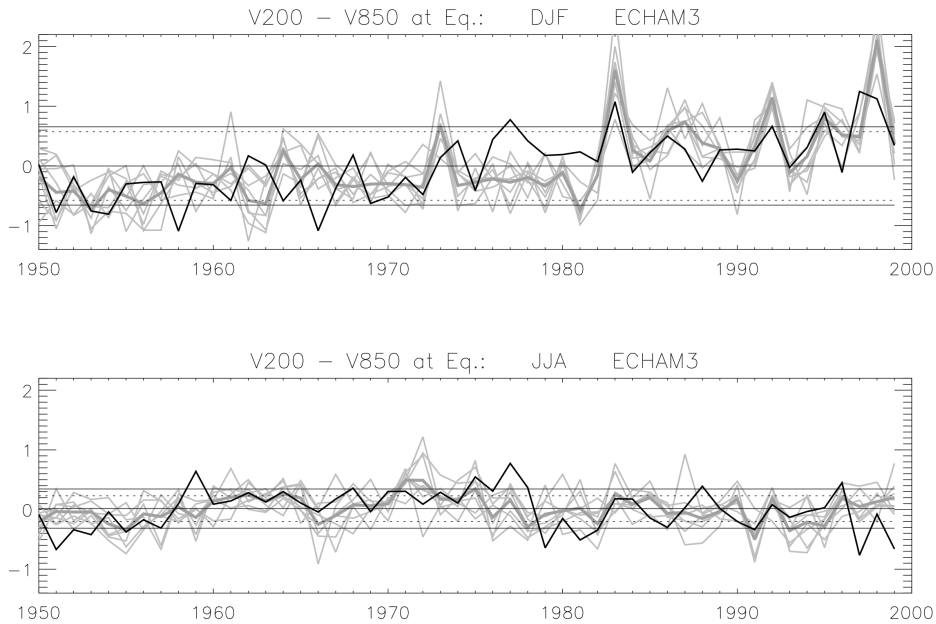


Figure 14. Time series of the vertical shear of the 200 hPa and 850 hPa zonal mean meridional wind: DJF (top panel) and JJA (bottom panel) over the equator. The gray thick solid curves represent the ensemble average, and gray thin dotted curves for each individual simulation. The standard deviation due to the temporal variation in the ensemble average is indicated by the distance between dashed line and the line of average. The standard deviation that includes inter-sample differences is represented by the solid-lines at outside of the dashed lines. The black solid curves show the vertical wind shear in NCEP reanalysis.

The regional patterns of the simulated epochal changes in winter and summer 200 hPa divergent mass circulations are shown in Figure 16. The oceanic warming, through its forcing of increased oceanic rainfall, intensifies winter regional monsoon circulations over the Indian Ocean and western Pacific region. We speculate that the intensified divergent mass circulation over the equatorial eastern Pacific in recent decades is related to the larger, more frequent El Niños of recent years (Fig. 16, top panel), further evidence for which will be given in next section. Note the strong zonal symmetry of the increased poleward mass transport at 200 hPa during winter, a structure projecting on the zonally symmetric Hadley cell. During the northern summer, the oceanic warming forces intensification of convection over mainly the western Pacific Ocean, which appears to be coupled with the intensification of descending motion in the tropics, for example over North Africa and over the northern tropical American monsoon area. It is also noticed that the upper level divergent flow over the Southern Hemisphere is stronger than over the Northern Hemisphere during the summer, which may be attributed to weaker SST cooling in the southern extratropics compared to the strong SST cooling in the northern extratropics (e.g., Parker et al 1994; also see Fig.8 in Quan et al. 2003).

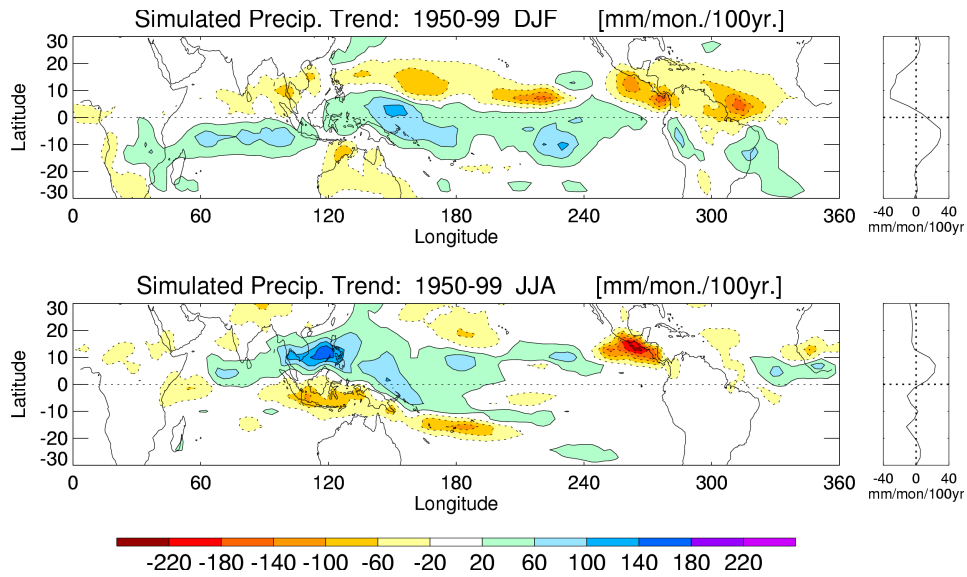


Figure 15. Linear trend in the ensemble average of the ECHAM3 simulated precipitation for the period of 1950-99 during DJF (top panel) and JJA (bottom panel). Zonal means of the trend are shown in the panels on right-hand side.

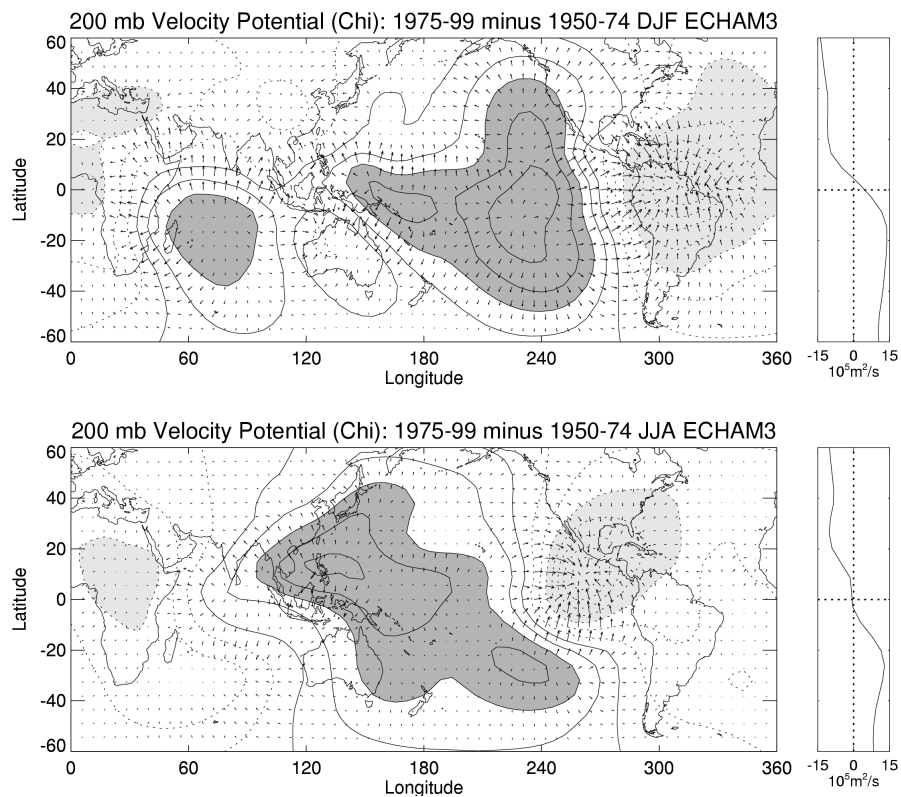


Figure 16. Change in the ensemble mean of the ECHAM3 200 hPa divergence wind field for DJF (top panel) and JJA (bottom panel). Contours for the velocity potential fields start from  $(\pm) 5 \times 10^5 \text{ m}^2 \text{ s}^{-1}$  with contour interval of  $10^5 \text{ m}^2 \text{ s}^{-1}$ . Dark/light shades indicate areas where the velocity potentials are higher/lower than  $\pm 25 \times 10^5 \text{ m}^2 \text{ s}^{-1}$ . Zonal means of the velocity potential differences are shown in the panels on the right-hand side.

### 4.3 The role of the warming trend of tropical “warm pool” SSTs

The mean warming of the tropical oceans also appears to be an important factor that contributes to the intensification of the tropical Hadley cell during the Northern Hemisphere winter. To demonstrate this impact, the DJF intensification of the Hadley cell simulated by the ECHAM3 model can be partitioned into ENSO-related and non-ENSO-related portions. Figure 17 (left panel) shows the time series of the linear regression between the Hadley cell index and the spatial average of SST anomalies for the region (15°S–15°N, 160°W–80°W, see top panel in Fig. 2). The residual from this linear regression (i.e. total value minus regressed value) is shown in the right panel in Figure 17. About half of the DJF intensification of the Hadley cell can be explained by the linear response to the increased amplitude of El Niño in the central and eastern tropical Pacific Ocean. The remaining part is non-ENSO in origin, of which we believe the most relevant oceanic change to be the mean state, especially the warming over the tropical Indian and western Pacific Oceans as indicated further below.

As has already been shown, the temporal change in Hadley cell intensity since 1950 has been linked with an intensification of the tropical hydrological cycle. Manifestations of the enhanced hydrological cycle include, during northern winter, the increased southern tropical rainfall together with northern tropical drying, and a reversed rainfall pattern during summer (lower panel, Figs. 11 and 13). One contribution to the Hadley cell change that we have emphasized is the change in statistical properties of El Niño. This is further shown in Figure 18 (top panel), which shows the substantial increase in equatorial Pacific rainfall response to the El Niño’s occurring after 1970, as simulated by the ECHAM3 model. The effect on the Hadley circulation is clearly seen in the time history of the ENSO contribution to the Hadley cell (left panel in Fig. 17). On the other hand, the right-side panel in Figure 17 appears to be more driven by the increase in warm-pool precipitation that is especially evident after 1980 (Fig. 18, bottom panel). This trend toward increased rainfall—evident in both models and observations—had previously been documented, and is consistent with the underlying SST warming (e.g., Hoerling et al. 2001a; Hurrell et al. 2004; Hoerling et al. 2004).

Hadley Circulation Index: Zonal Ave. V200 – V850 by ECHAM3

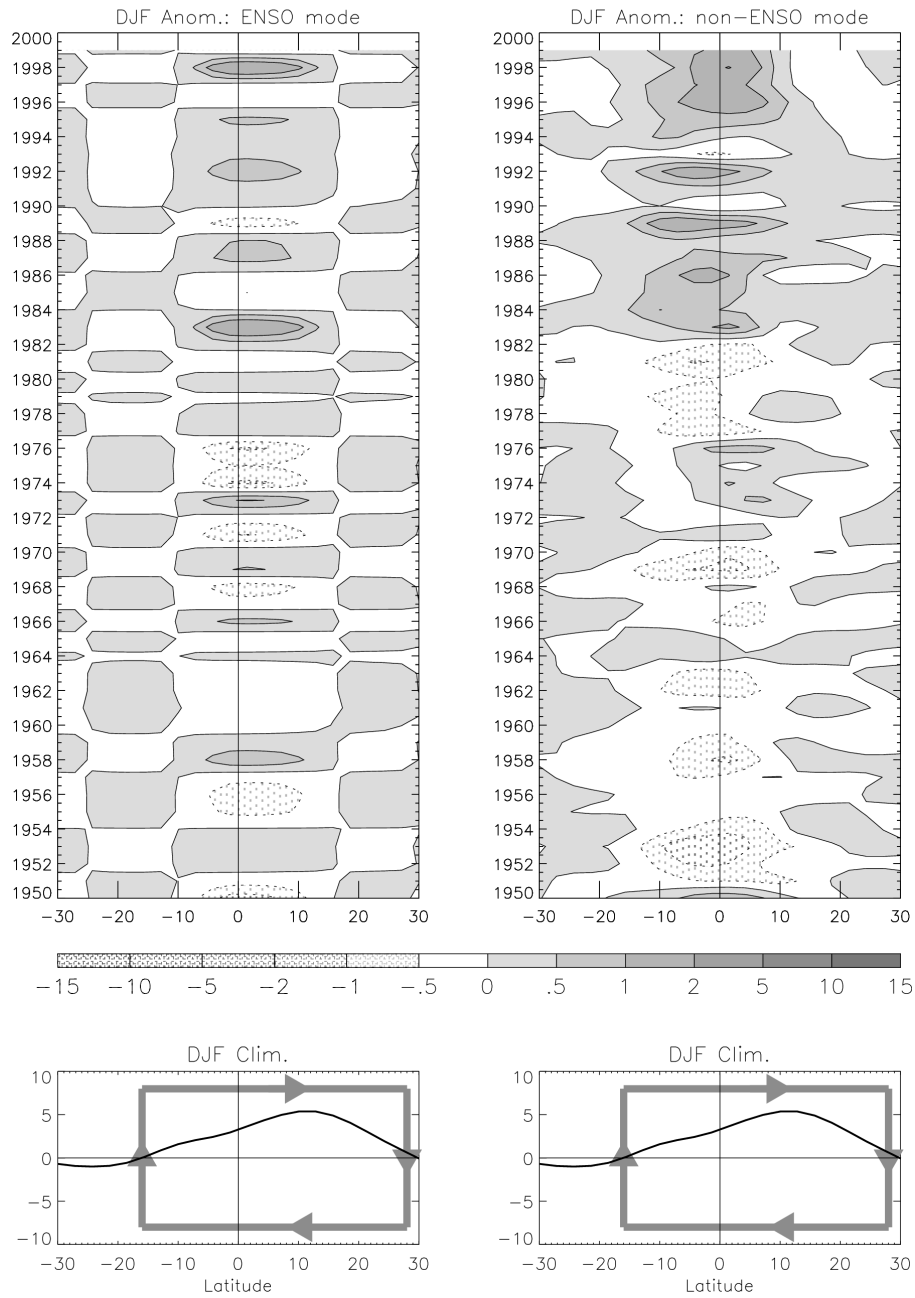


*Figure 17.* Time-latitude cross-section of the DJF anomalous zonal mean vertical shear between the meridional wind at 200 hPa and 850 hPa (V200 minus V850) in the ensemble mean of the ECHAM3 simulations for the ENSO component (left panel) and the residual (right panel), respectively. The climatological means of the zonal mean vertical wind-shear for DJF are shown in the bottom two panels with the schematic arrows interpreting the meaning of the positive/negative signs of the values.

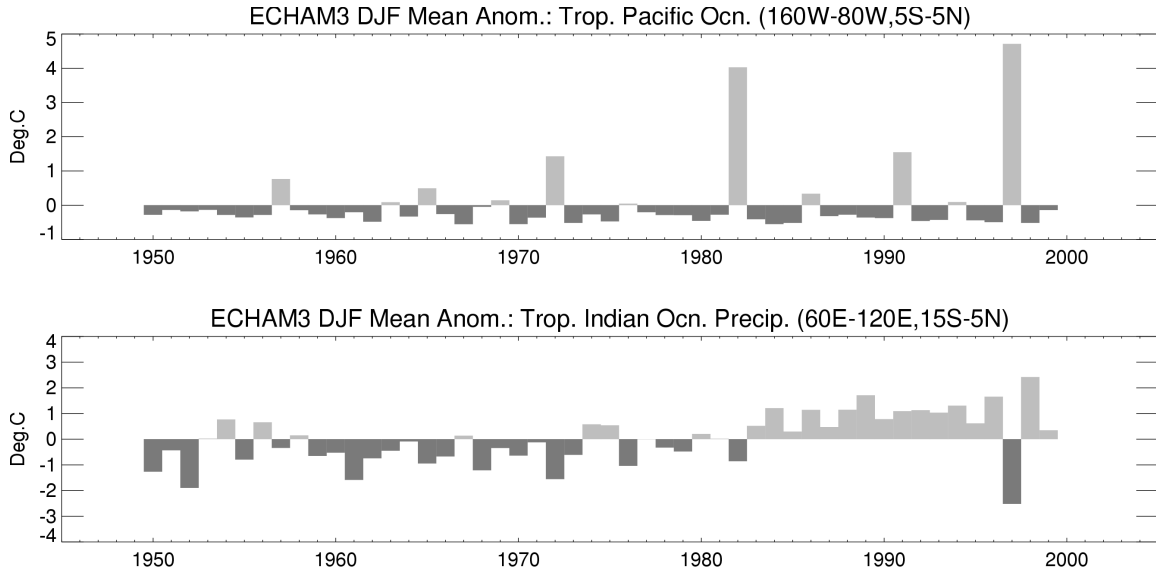


Figure 18. Time series of DJF mean anomalous precipitation in the ensemble mean of the ECHAM3 simulations.

For the recent decades, for which independent observational data is available, we have compared the simulated precipitation with satellite precipitation estimates over the open oceans. Figure 19 shows a comparison between the model-simulated precipitation and the observed precipitation from GPCP. The top panel shows the time series of the spatial average of 3-month mean precipitation in the tropical zone ( $10^{\circ}\text{S}$ – $10^{\circ}\text{N}$ ) for the Northern Hemispheric winter. The model simulation shows a reasonable agreement with the observations for interannual variations during the 1980–1999 period. To verify the model’s amplitude of rainfall variations in response to the tropical SST, we compare the composite amplitude of anomalous precipitation of the GPCP data with that of the model simulation in the lower panel of Figure 19. The composite anomalies are made from the DJF of 1982/83, 1986/87, and 1997/98 for the warm events, and January-February 1980, 1988/89 DJF, and December of 1999 for the cold events (cf. the SST time series in the middle panel of Fig. 19). The amplitude of the model simulated rainfall anomalies are comparable to the observations. We note that the increase of rainfall over the tropical Pacific Ocean is consistent with a study by Morrisey and Graham (1996).

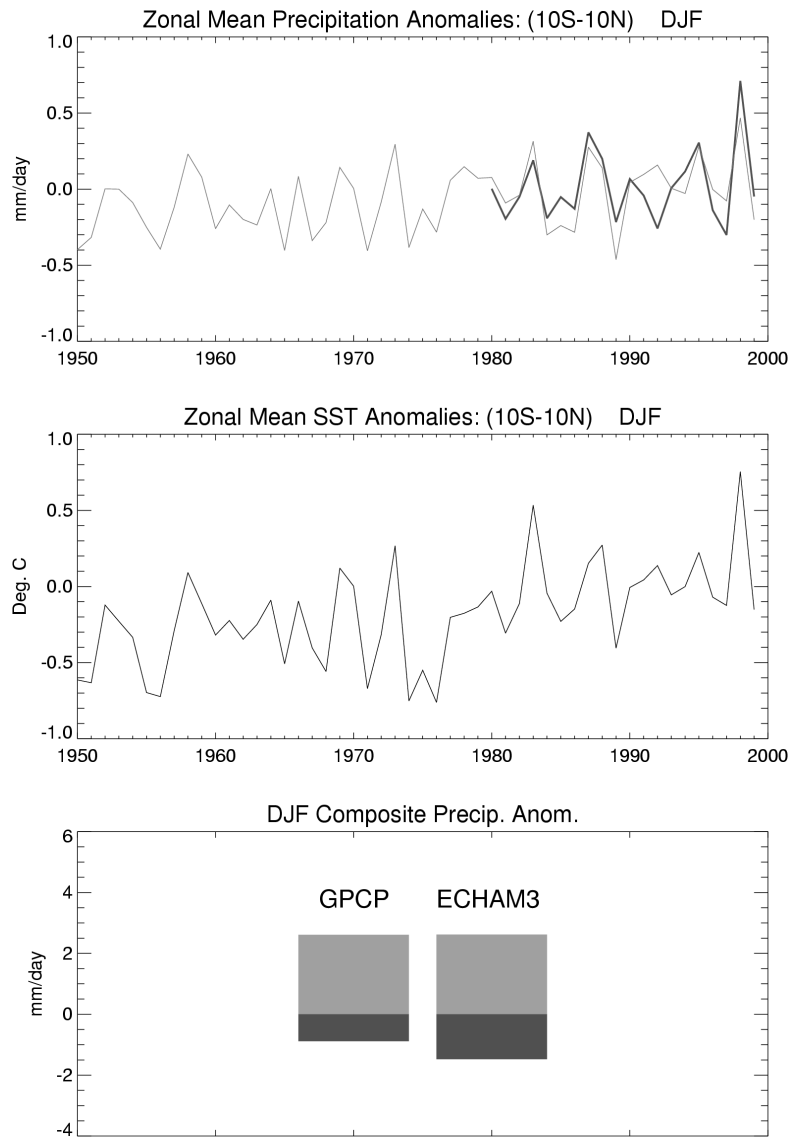


Figure 19. Time series of the spatial mean of the DJF anomalous precipitation over the global tropical zone (10°S–10°N) in the ensemble mean of the ECHAM3 simulation (thin line, top-panel), the GPCP observations (dark line, top-panel), and the DJF anomalous SST (middle-panel). The values of composite anomalous rainfall are compared in the bottom-panel for El Niño (grey)/ La Niña (black) for the GPCP observation (left side) and the ECHAM3 ensemble mean.

## 5. Summary and Discussion

The consistent results emerging from our analyses of the reanalysis and model simulations suggest the following conclusions:

- The winter (DJF) Hadley cell has increased in intensity since 1950.
- The temporal variation of the tropical Hadley cell during 1950–99 is closely

related to the variation of the sea surface temperatures in the tropical oceans. At interannual time-scales, the tropical Hadley cell is linked to the interannual variation of El Niño-Southern Oscillation (ENSO). The Hadley cell responds particularly strongly to the El Niño events, but more weakly to the La Niña events. There are also non-linear differences between the spatial structures in the Hadley cells' responses to the opposite phases of ENSO. The change in statistical properties of ENSO since 1950, in particular the increased frequency and amplitude of El Niño events since 1976, have contributed to a strengthening trend of the NH winter Hadley cell.

- The warming in the tropical Indo-west Pacific warm-pool is an equally important forcing factor that has been driving an acceleration of the boreal winter Hadley cell.
- The time history of the southward overturning Hadley cell during the Southern Hemispheric winter lacks a trend, though it does exhibit strong decadal variations.
- A strong seasonal dependence of the 50-year trend in the tropical Hadley cell reflects different impacts of tropical SST warming trends on the oceanic-dominated monsoons during the northern winter versus the continental-dominated monsoons during the southern winter.

The analysis revealed a substantial non-linearity in the Hadley-cell/ENSO connection. A possible cause is the non-linearity in thermodynamic processes that determines the strength of rainfall response to the interannual variation in the tropical Pacific SST. In particular, a warm SST anomaly may cause larger rainfall and diabatic heating changes than an equal cold SST anomaly (e.g. Zhang 1993). To the extent that there exists a zonal mean component to this rainfall response, thermodynamic non-linearity offers one possible explanation for why the Hadley cells' response to the cold ENSO events is weaker than its counterpart to the warm ENSO events. Global circulation impacts from such a thermodynamic non-linearity have been found in the ENSO-PNA teleconnection (Hoerling et al. 2001b), and in the seasonal cycle of atmospheric climate predictability (Quan 1998; Quan et al. 2004).

Another possible explanation for the non-linearity in the Hadley-cell/ENSO connection is the difference in the geographical location of the maximum rainfall anomalies associated with warm versus cold ENSO state. A study by Hoerling et al. (1997) showed that the maximum rainfall anomalies along the equator are located east of the dateline during warm ENSO events, but west of the dateline during the cold events, implying large differences in diabatic heating patterns associated with the two extreme ENSO phases (e.g. DeWeaver and Nigam, 2002). Taking into account the existence of the Walker Circulation, spatial structure of atmospheric response to the anomalous rainfall/diabatic heating in the ascending branch of the Walker Circulation (west of dateline) is not a linear reverse to its counterpart responding to anomalous forcing in the descending branch (east of the dateline), neither the spatial pattern of the Hadley cell change in the cold ENSO events to the pattern of the Hadley cell change during the warm

ENSO events.

As indicated in the above analyses, the tropical Hadley cells have responded to the interannual variations of ENSO quite differently before and after the mid-1970s. This interdecadal change in the tropical Hadley cells' response to ENSO describes one aspect of a regime-change in the global atmospheric circulation after the mid-1970s. Other aspects of the regime-change in the global atmospheric circulation have been found by previous authors, and include (1) the intensification of cyclones over the North Pacific Ocean during the Northern Hemispheric winter (e.g. Graham and Diaz 2001); (2) a phase- change in the preferred interannual occurrence of the North Atlantic Oscillation (e.g. Hurrell 1995; Thompson et al. 2000); (3) a weakened correlation between the Indian Monsoon and ENSO during the Northern Hemispheric summer (e.g. Kumar et al 1999; Kingster III et al. 2002); (4) a change in the correlation between ENSO and interannual swings of Australian monsoon rainfall (Power et al. 1999); (5) change in the onset process of ENSO over the tropical Pacific Ocean (Wang 1995).

The change of the tropical Hadley cell is dynamically consistent with the intensification of cyclones over the North Pacific, and each is further consistent with the change in ENSO statistics. The enhanced northward overturning cell during El Niño events after 1976 contributes to an intensification of the westerlies over the subtropical North Pacific, which in turn creates a more favorable vertical shear profile for cyclone intensification. On the other hand, the enhanced northward overturning Hadley cell lead to a stronger easterly (trade) wind flow in the tropics, consistent with the results by Wang (1995) who found the trade winds over the tropical south-east Pacific intensified during the onset phase of El Niño events occurring after 1976 compared to the earlier El Niños.

What is a possible cause for such regime-change in atmospheric circulation? Wang (1995) suggested that the regime change in the ENSO evolution is linked to the background warming of the eastern tropical Pacific Ocean. Our analyses of the regime-change of the tropical Hadley cell offers another plausible hypothesis for how the warming in the eastern tropical Pacific has led to the regime-change in the atmospheric circulation. The warming in the tropical eastern Pacific has occurred more rapidly in the area south side of the equator, especially during the Northern Hemispheric winter (Fig. 1). In response to the stronger warming in the southern tropical Pacific, the maximum rainfall anomalies shifted from the north side of the equator during the El Niño events before 1970's, to the south side of the equator after the 1970's (see Fig. 11 & 13). Because of the southward shift of the maximum anomalous rainfall, the northward overturning Hadley cell became more dominant during the El Niño events after the 1970's, which is further manifested by the intensification of the cyclones over the North Pacific and the trades over the tropical southeastern Pacific.

Another factor that may contribute to the regime-change of the tropical Hadley cell is the change in meridional SST gradient in the Pacific Ocean. The meridional SST gradient has been largely increased in the North Pacific Ocean by the warming in tropical Pacific and cooling in northern extratropical Pacific (e.g. Graham 1994; Trenberth and Hurrell 1994; Zhang et al. 1997). In contrast, change in the meridional SST gradient in the South Pacific Ocean is only moderate because the SST cooling in the southern extratropical Pacific has been much weaker than its counterpart in the northern extratropical Pacific (Parker et al. 1994). The increased tropical-to-extratropical SST gradient in the North Pacific provides a favorable condition for stronger southerly winds at lower

troposphere over the subtropical North Pacific and an intensified northward overturning Hadley cell during the northern winter, which in turn helps the persistence/development of the SST cooling in the northern extratropical Pacific (Lau and Nath 1996)—forming a positive feedback in the ocean-atmosphere-ocean coupled variation. The absence of a similar trend of intensified southward overturning Hadley cell during the Southern Hemispheric winter indicates that such kind of ocean-atmosphere feedback process has been much weaker or even not been exist over the South Pacific Ocean during the southern winter since 1950.

Some uncertainties still exist in the reanalysis-model comparison. A major uncertainty for the Northern Hemisphere winter season is the difference in the timing of the regime change in the tropical Hadley cell. The change occurred around the late 1960s to early 1970s (cf. the right panel in Fig. 10) in the reanalysis, but the late 1970s to early 1980s in the model simulation (the right panel in Fig. 12). The change in the tropical Indo-Pacific SST in the late 1970s seems to be a dominant factor in the model simulation. Some other process must have also been influential in the reanalysis in causing its change to occur in the late 1960s. One possible concern is the change in the quantity and spatial coverage of the observed data included in the reanalysis. A rapid increase in the total number of observations in the Southern Hemisphere took place in the mid- to late 1960s (Kistler et al. 2001), and the change in the spatial coverage might have caused a shift of the climate mean state of the Southern Hemispheric circulation in the reanalysis data around that time. However, some significant climate change did occur during the late 1960s. For example, a persistent drought in the tropical North Africa started to develop in the late-1960s, accompanied by a change in the north-south interhemispheric gradient of sea surface temperature in the Atlantic Ocean (e.g. Ward 1998). Additionally, the change in the Atlantic Ocean may also affect the circulation regime over the Indo-Pacific Oceans (e.g. Chang et al 2001). However, the uncertainty is larger for the boreal summer. The interdecadal change in the model simulated 200 hPa divergence wind field during the Northern Hemisphere summer (Fig. 16, bottom panel) is quite different compared to its counterpart in the reanalysis (e.g., Kumar et al. 1999; Krishnamurthy and Goswami 2000; Chang et al. 2001; Quan et al. 2003).

## References

- Chang, C.P., P. Harr, and J. Ju, 2001: Possible roles of Atlantic circulations on the weakening Indian Monsoon rainfall-ENSO relationship. *J. Climate*, **14**, 2376-2380.
- Chen, J., B.E. Carlson, and A.D. Genio, 2002: Evidence for strengthening of the tropical general circulation in the 1990s, *Science*, **295**, 838-841.
- DeWeaver, E. and S. Nigam, 2002: Linearity in ENSO's atmospheric response. *J. Climate*, **15**, 2446-2461.
- Diaz, H.F., C.B., Fu, and X.W. Quan, 1992: A comparison of surface geostrophic winds with COADS ship wind observations. *Proceedings of the International COADS Workshop, Boulder, Colorado, 13-15 January 1992*, 131-141.
- Diaz, H.F., X.W. Quan, C.B. Fu, 1994: Marine surface wind changes during 1978-1992: an estimation based on COADS. *Proceedings of the International COADS Winds Workshop, Kiel, Germany, 31 May – 2 June, 1994*, 48-67.

- Dima, I., and J. M. Wallace, 2003: On the seasonality of the Hadley Cell. *J. Atmos. Sci.*, **60**, 1522-1527.
- Gaffen, D. J., B. D. Santer, J.S. Boyle, J. R. Christy, N.E. Graham, and R. J. Ross, 2000: Multidecadal changes in the vertical temperature structure of the tropical troposphere. *Science*, **287**, 1242-1245.
- Graham, N.E., 1994: Decadal-scale climate variability in the tropical and north Pacific during the 1970s and 1980s: observations and model results, *Clim. Dyn.*, **10**, 135-162.
- Graham, N. E., T. P. Barnett, R. Wilde, M. Ponater, and S. Schubert, 1994: On the role of tropical and midlatitudes SSTs in forcing interannual to interdecadal variability in the winter northern hemisphere circulation. *J. Climate*, **9**, 1416-1441.
- Graham, N.E., H.F. Diaz, 2001: Evidence for intensification of North Pacific winter cyclones since 1948. *Bull. Amer. Meteor. Soc.*, **82**, 1869-1893.
- Hoerling, M. P., A. Kumar, and M. Zhong, 1997: El Niño, La Niña, and the nonlinearity of their teleconnections. *J. Climate*, **10**, 1769-1786.
- Hoerling, M.P., J.W. Hurrell, and T. Xu, 2001a: Tropical origins for recent north Atlantic climate change, *Science*, **292**, 90-92.
- Hoerling, M. P., A. Kumar, and T. Xu, 2001b: Robustness of the nonlinear climate response to ENSO's extreme Phases. *J. Climate*, **14**, 1277-1293.
- Hoerling M.P., J. W. Hurrell , T. Xu , G. T. Bates, and A. Phillips, 2004: Twentieth Century North Atlantic climate change. Part II: Understanding the effect of Indian Ocean warming. *Climate Dyn. (in press)*.
- Huang, H. P., K. M. Weickmann, and C. J. Hsu, 2001: Trend in atmospheric angular momentum in a transient climate change simulation with greenhouse gas and aerosol forcing. *J. Climate*, **14**, 1525-1534.
- Huang, H.P., K.M. Weickmann, and R.D. Rosen, 2003: Unusual behavior in atmospheric angular momentum during the 1965 and 1972 El Niños. *J. Climate*, **16**, 2526-2539.
- Hurrell, J. 1995: Decadal trends in the North Atlantic Oscillation: regional temperature and precipitation. *Science*, **269**, 676-679.
- Hurrell, J. 1996: Influence of variations in extratropical wintertime teleconnections on Northern Hemisphere temperature. *Geophys. Res. Lett.*, **23**, 665-668.
- Hurrell J.W., M. P. Hoerling, A. Phillips, and T. Xu, 2004: Twentieth Century North Atlantic climate change. Part I: Assessing determinism. *Climate Dyn. (in press)*
- IPCC, 1996: *Climate Change 1995: The Science of Climate Change*. J.T. Houghton et al. (eds.), Cambridge University Press, 572 pp.
- IPCC, 2001: *Climate Change 2001: The Science Basis*. J.T. Houghton et al. (eds.), Cambridge University Press, 881 pp.
- Jones, P.D., M. New, D.E. Parker, S. Martin, and I.G. Rigor, 1999: Surface air temperature and its changes over the past 150 years. *Rev. Geophys.*, **37**, 173-199.
- Kinister III, J. L., K. Miyakoda, and S. Yang, 2002: Recent change in the connection from the Asian Monsoon to ENSO. *J. Climate*, **15**, 1203-1215.
- Kistler, R., E. Kalnay, W. Collins, S. Saha, G. White, J. Woollen, M. Chelliah, W. Ebisuzaki, M. Kanamitsu, H. van den Dool, R. Jenne, and M. Fiorino, 2001: The NCEP/ NCAR 50-year reanalysis: monthly means, CD-ROM and documentation. *Bull. Amer. Meteorol. Soc.*, **82**, 152-168.
- Knutson, T.R., T.L. Delworth, K.W. Dixon, and R.J. Stouffer, 1999: Model assessment of regional temperature trends. *J. Geophys. Res.*, **104**, 30,981-30,996.
- Krishnamurthy, V., and B.N. Goswami, 2000: Indian monsoon-ENSO relationship on interdecadal timescale. *J. Climate*, **13**, 579-595.
- Kumar, A., F. Yang, L. Goddard, and S. Schubert, 2004: Differing trends in the tropical surface temperatures and precipitation over land and oceans. *J. Climate*, **17**, 653-664.

- Kumar, K.K., B. Rajagopalan, and M.A. Cane, 1999: On the weakening relationship between the Indian monsoon and ENSO. *Science*, **284**, 2156-2159.
- Latif, M., R. Kleeman, and C. Eckert, 1997: Greenhouse warming, decadal variability, or El Niño? An attempt to understand the anomalous 1990s. *J. Climate*, **10**, 2221-2239.
- Lau, K.-M., H. Weng, 1999: Interannual, decadal-interdecadal, and global warming signals in sea surface temperature during 1955-1997, *J. Climate*, **12**, 1257-1267.
- Lau, N.C., and M.J. Nath, 1994: A modeling study of the relative roles of tropical and extratropical SST anomalies in the variability of the global atmosphere-ocean system. *J. Climate*, **7**, 1184-1207.
- Lau, N.C., and M.J. Nath, 1996: The role of the “atmospheric bridge” in linking tropical Pacific ENSO events to extratropical SST anomalies. *J. Climate*, **9**, 2036-2057.
- Levitus, S., J. Antonov, T.P. Boyer, C. Stephens, 2000: Warming of the world ocean, *Science*, **287**, 2225-2229.
- Oort, A.H., and J.J. Yienger, 1996: Observed interannual variability in the Hadley circulation and its connection to ENSO, *J. Climate*, **9**, 2751-2767.
- Parker, D.E., P.D. Jones, C.K. Folland, and A. Bevan, 1994: Interdecadal changes of surface temperature since the late nineteenth century. *J. Geophys. Res.* **99**, 14,373-14,399
- Parker, D. E., 2000: Temperatures High and Low, *Science*, **287**, 1216.
- Philander, S., G., 1990: *El Niño, La Niña, and the Southern Oscillation*. Academic Press, San Diego, 293 pp.
- Power, S., T. Casey, C. Folland, A. Colman, and V. Mehta, 1999: Inter-decadal modulation of the impact of ENSO on Australia. *Climate Dyn.*, **15**, 319-324.
- Quan, X.W., 1998: Interannual variability associated with ENSO: seasonal dependence and interdecadal change. Ph.D Thesis, University of Colorado at Boulder.
- Quan, X.W., H. F. Diaz, and C. B. Fu, 2003: Interdecadal change in the Asian-Africa summer monsoon and its associated changes in global atmospheric circulation. *Global and Planetary Change*, **37**, 171-188.
- Quan, X.W., P. J. Webster, A. M. Moore, and H. R. Chang, 2004: Causes of the seasonality in SST forced atmospheric short-term climate predictability. *J. Climate*, (in press).
- Roeckner, E. and Coauthors, 1992: Simulation of the present-day climate with the ECHAM model: Impact of model physics and resolution. *Max-Planck-Institute für Meteorologie Rep.*, **93**, 171 pp. [Available from MPI für Meteorologie, Bundesstr. 55, D-20146 Hamburg, Germany.]
- Santer, B. D., T. M. Wigley, D.J. Gaffen, L. Bengtsson, C. Doutriaux, J. S. Boyle, M. Esch, J.J. Hnilo, P. D. Jones, G. A. Neel, E. Roeckner, K. E. Taylor, M. F. Wehner, 2000: Interpreting differential temperature trends at the surface and the lower troposphere. *Science*, **287**, 1227-1231.
- Smith, T.M., R.W. Reynolds, R.E. Livezey, and D.C. Stokes, 1996: Reconstruction of historical sea surface temperature using empirical orthogonal functions. *J. Climate*, **9**, 1402- 1420.
- Thompson, D.W.J., J.M. Wallace, and G.C. Hegerl, 2000: Annular modes in the extratropical circulation. part II: trends. *J. Climate*, **13**, 1018-1036.
- Trenberth, K.E., and J.W. Hurrell, 1994: Decadal atmosphere-ocean variations in the Pacific, *Clim. Dyn.*, **9**, 303-319.
- Trenberth, K.E., G.W. Branstator, D. Karoly, A. Kumar, N.-C. Lau, and C. Ropelewski, 1998: Progress during TOGA in understanding and modeling global teleconnections associated with tropical sea surface temperatures. *J. Geophys. Res.*, **103**, 14 291-14 324.
- Trenberth, K.E., D.E. Stepaniak, and J.M. Caron, 2000: The global monsoon as seen through the divergent atmospheric circulation, *J. Climate*, **13**, 3969-3993.
- Trenberth, K.E., 2002: Changes in tropical clouds and radiation, *Science*, **296**, 2095.
- Waliser, D.E., Z. Shi, J.R. Lanzante, A.H. Oort, 1999: The Hadley circulation: assessing NCEP/NCAR reanalysis and sparse in-situ estimates, *Clim. Dyn.*, **15**, 719-735.

- Wang, B., 1995: Interdecadal change in El Niño onset in the last four decades. *J. Climate*, **8**, 267-285.
- Ward, M.N., 1998: Diagnosis and shot-lead time prediction of summer rainfall in tropical North Africa at interannual and multidecadal timescales. *J. Climate*, **11**, 3167-3191.
- Webster, P. J., 1987: The elementary monsoon. *Monsoons*, J.S. Fein and P.L. Stephens (eds.), John Willey & Sons, New York, 3-32.
- Zhang, C. D., 1993: Large-scale variability of atmospheric deep convection in relation to sea surface temperature in the tropics. *J. Climate*, **6**, 1898-1913.
- Zhang, Y., J. M. Wallace, and D.S. Battisti, 1997: ENSO-like interdecadal variability: 1900-93. *J. Climate*, **10**, 1004-1020.